

# Direct Least Square Fitting of Paracatadioptric Line Images

Joao P. Barreto

Institute of Systems and Robotics  
Dept. of Electrical and Computer Engineering  
University of Coimbra  
3030 Coimbra - PORTUGAL  
jpbar@isr.uc.pt

Helder Araujo

Institute of Systems and Robotics  
Dept. of Electrical and Computer Engineering  
University of Coimbra  
3030 Coimbra - PORTUGAL  
helder@isr.uc.pt

## Abstract

*Paracatadioptric sensors combine a parabolic shaped mirror and a camera inducing an orthographic projection. Such a configuration provides a wide field of view while keeping a single effective viewpoint. In general the paracatadioptric image of a line is a conic curve. The estimation of line images is an important subject for applications such as reconstruction and visual control of motion. However the estimation of the conic curves where lines are mapped is hard to accomplish. In general only a small arc of the conic is visible in the image and conventional conic fitting techniques are unable to correctly estimate the curve. This paper shows that line images can be accurately estimated by constraining the search space. A conic curve is the paracatadioptric image of a line if, and only if, the image of the circular points lie on the curve and two certain points are conjugate with respect to the conic. Considering the space of all conic curves, the line images lie in a linear subspace which depends on the system calibration. The paracatadioptric projection of a line can be estimated by fitting a conic in the subspace to the data points. The proposed approach is computationally efficient since the fitting problem can be solved by an eigensystem*

## 1 Introduction

The approach of combining mirrors with conventional cameras to enhance sensor field of view is referred to as catadioptric image formation. The use of catadioptric systems to achieve panoramic vision is simple and fast enabling the capture of dynamic scenes. The entire class of catadioptric configurations verifying the fixed viewpoint constraint is derived in [1]. Panoramic central catadioptric systems can be built by combining an hyperbolic mirror with a perspective camera and, a parabolic mirror with an orthographic camera (paracatadioptric sensor). The construction of the former requires a careful alignment between the mirror and

the imaging device. The camera projection center must be positioned in the outer focus of the hyperbolic reflective surface. The paracatadioptric camera is easier to construct being broadly used in applications requiring omnidirectional vision.

The paracatadioptric image formation can be modeled by a stereographic projection from a sphere, centered in the effective viewpoint, into a plane [2]. The plane and the final catadioptric image are related by a collineation depending on the mirror parameters and camera intrinsic matrix. For the particular case of a parabolic system this projective transformation is always affine. The system is calibrated whenever the collineation is known. The calibration can be performed using the image of three or more lines in general position in the world as explained in [3]. The paracatadioptric sensor maps a line in the world into a conic curve in the image plane [2]. In general only a small arc of the conic locus is visible in the image and conventional conic fitting techniques are unable to correctly estimate the curve [6].

The present paper proposes a conic fitting algorithm that copes with the occlusion problem and accurately estimates paracatadioptric line images. The approach is specific for line projection in a parabolic system and assumes that the sensor is calibrated. If it is true that any line maps into a conic, it is not true that any conic is the image of a line. We prove that a conic curve is the paracatadioptric image of a line if, and only if, the image of the circular points lie on the curve and two certain points are conjugate with respect to the conic. The paracatadioptric camera maps lines in the scene into conic curves which belong to a linear subspace in the space of all conics. By constraining the search space the line image can be accurately determined. The corresponding locus is estimated by fitting a conic in the subspace to the data points. The approach is computationally efficient since the fitting problem can be solved by an eigensystem. The proposed algorithm can be useful for many applications such as 3D reconstruction and visual control of motion using paracatadioptric images.

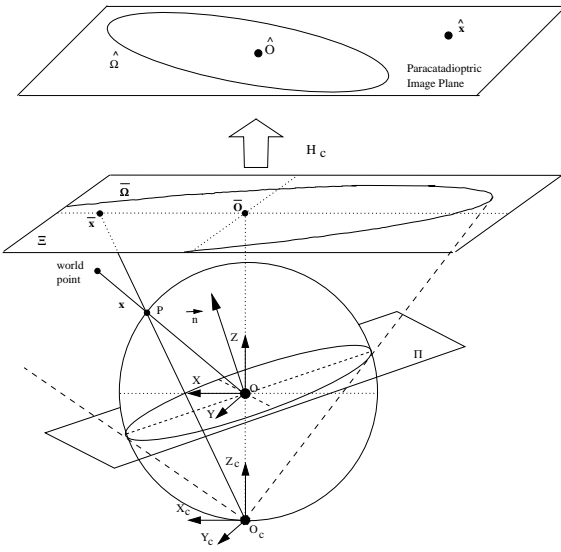


Figure 1: Model for paracatadioptric image formation

## 2 The Paracatadioptric Camera

This section reviews the image formation model for paracatadioptric systems [2] and introduces the necessary and sufficient conditions for a conic curve being the paracatadioptric image of a line.

### 2.1 The Mapping Model

Assume a paracatadioptric system combining a parabolic mirror with latus rectum  $4p$ , and an orthographic camera. The principal axis of the camera must be aligned with the symmetry axis of the paraboloid. The paracatadioptric projection can be modeled by a stereographic projection from an unitary sphere, centered in the effective viewpoint, into a plane  $\Xi$  as shown in Fig. 1.

The world point shown in Fig. 1 is imaged at point  $\hat{x}$  in the paracatadioptric image plane. The mapping can be described as follows. To each visible scene point corresponds an oriented projective ray  $x = (x, y, z)^t$ , joining the 3D point with the projection center  $\mathbf{O}$ . The projective ray intersects the unit sphere in a single point  $\mathbf{P}$ . Consider a point  $\mathbf{O}_c$ , with coordinates  $(0, 0, -1)^t$ , which lies in the unitary sphere. To each  $x$  corresponds an oriented projective ray  $\bar{x}$  joining  $\mathbf{O}_c$  with the intersection point  $\mathbf{P}$ . The non-linear mapping  $\mathbf{F}$  (equation 1) corresponds to projecting the scene in the unity sphere surface and then re-projecting the points on the sphere into a plane  $\Xi$  from a novel projection center  $\mathbf{O}_c$ . Points in catadioptric image plane  $\hat{x}$  are obtained after a collineation  $\mathbf{H}_c$  of 2D projective points  $\bar{x}$ . Equation 2 shows that  $\mathbf{H}_c$  depends on the intrinsic parameters  $\mathbf{K}_c$  of the orthographic camera, and on the latus rectum of the

parabolic mirror.

$$\mathbf{F}(\mathbf{x}) = (x, y, z + \sqrt{x^2 + y^2 + z^2})^t \quad (1)$$

$$\hat{\mathbf{x}} = \mathbf{K}_c \underbrace{\begin{bmatrix} 2p & 0 & 0 \\ 0 & 2p & 0 \\ 0 & 0 & 1 \end{bmatrix}}_{\mathbf{H}_c} \bar{\mathbf{x}} \quad (2)$$

Consider the plane  $\Pi = (\mathbf{n}, 0)^t$  going through the effective viewpoint  $\mathbf{O}$  as depicted in Fig. 1 ( $\mathbf{n} = (n_x, n_y, n_z)^t$ ). The paracatadioptric image of any line lying on  $\Pi$  is the conic curve  $\bar{\Omega}$ . The line in the scene is projected into a great circle in the sphere surface. This great circle is the curve of intersection of plane  $\Pi$ , containing both the line and the projection center  $\mathbf{O}$ , and the unit sphere. The projective rays  $\bar{x}$ , joining  $\mathbf{O}_c$  to points in the great circle, form a central cone surface. The central cone, with vertex in  $\mathbf{O}_c$ , projects into the conic  $\bar{\Omega}$  in plane  $\Xi$  (equation 3). Since the image plane and  $\Xi$  are related by collineation  $\mathbf{H}_c$ , the result of equation 4 comes in a straightforward manner. Notice that conic  $\bar{\Omega}$  is degenerated whenever  $n_z = 0$ . If the line is co-planar with the principal axis of the orthographic camera then the corresponding paracatadioptric image is also a line.

$$\bar{\Omega} = \begin{bmatrix} -n_z^2 & 0 & n_x n_z \\ 0 & -n_z^2 & n_y n_z \\ n_x n_z & n_y n_z & n_z^2 \end{bmatrix} \quad (3)$$

$$\hat{\Omega} = \begin{bmatrix} a & b & d \\ b & c & e \\ d & e & f \end{bmatrix} = \mathbf{H}_c^{-t} \bar{\Omega} \mathbf{H}_c^{-1} \quad (4)$$

### 2.2 The Image of a Line

Consider the scheme of Fig. 1 for the mapping of a line by a paracatadioptric sensor. Plane  $\Pi$ , containing both the line and the effective viewpoint  $\mathbf{O}$ , intersects the sphere in a great circle. The mapping from the sphere to plane  $\Xi$  is a stereographic projection. The stereographic projection maps any circle in the sphere into a circle in the plane [7]. Thus the great circle is projected into  $\bar{\Omega}$  which is circle as can be verified by inspecting equation 3. Points in plane  $\Xi$  are mapped into points in the image by a collineation  $\mathbf{H}_c$ . Notice that for the parabolic situation  $\mathbf{H}_c$  is always an affine transformation (equation 2). Since an affine transformation does not change the type of conic, then the paracatadioptric image of a line  $\hat{\Omega}$  is always a circle/ellipse (equation 4).

Consider the following points lying on plane  $\Xi$ :  $\bar{\mathbf{I}} = (1, i, 0)^t$ ,  $\bar{\mathbf{J}} = (1, -i, 0)^t$ ,  $\bar{\mathbf{G}} = (1, 0, -i)^t$  and  $\bar{\mathbf{H}} = (1, 0, i)^t$ . Points  $\bar{\mathbf{I}}$  and  $\bar{\mathbf{J}}$  are the circular points of the plane. It is well known that any circle must go through the circular points. Since  $\bar{\Omega}$  is always a circle, then it is true that  $\bar{\mathbf{I}}^t \bar{\Omega} \bar{\mathbf{I}} = 0$  and  $\bar{\mathbf{J}}^t \bar{\Omega} \bar{\mathbf{J}} = 0$ . Moreover from equation 3 arises

that  $\bar{\mathbf{G}}^t \bar{\Omega} \bar{\mathbf{H}} = 0$ . Points  $\bar{\mathbf{G}}$  and  $\bar{\mathbf{H}}$  are conjugate with respect to the conic curve  $\bar{\Omega}$ . Assume that collineation  $\mathbf{H}_c$  maps points  $\bar{\mathbf{I}}, \bar{\mathbf{J}}, \bar{\mathbf{G}}$  and  $\bar{\mathbf{H}}$  into points  $\hat{\mathbf{I}}, \hat{\mathbf{J}}, \hat{\mathbf{G}}$  and  $\hat{\mathbf{H}}$ .

**Proposition:** A conic curve  $\hat{\Omega}$  is the paracatadioptric image of a line in the scene if, and only if, it contains points  $\hat{\mathbf{I}}$  and  $\hat{\mathbf{J}}$  ( $\hat{\mathbf{I}}^t \hat{\Omega} \hat{\mathbf{I}} = 0$ ,  $\hat{\mathbf{J}}^t \hat{\Omega} \hat{\mathbf{J}} = 0$ ), and points  $\hat{\mathbf{G}}, \hat{\mathbf{H}}$  are conjugate with respect to  $\hat{\Omega}$  ( $\hat{\mathbf{G}}^t \hat{\Omega} \hat{\mathbf{H}} = 0$ ).

*Proof:* The circle  $\bar{\Omega}$  must go through the circular points  $\bar{\mathbf{I}}, \bar{\mathbf{J}}$ . Since collineation  $\mathbf{H}_c$  preserves incidence, then both points  $\hat{\mathbf{I}}, \hat{\mathbf{J}}$  lie on the parabolic line image  $\hat{\Omega}$ . Moreover the projective transformation also preserves the cross-ratio and pole/polar relations. Since points  $\bar{\mathbf{G}}, \bar{\mathbf{H}}$  are conjugate with respect to  $\bar{\Omega}$ , then  $\hat{\mathbf{G}}, \hat{\mathbf{H}}$  are also conjugate with respect to  $\hat{\Omega}$ . Thus, if  $\hat{\Omega}$  is a paracatadioptric line image, then it must verify  $\hat{\mathbf{I}}^t \hat{\Omega} \hat{\mathbf{I}} = 0$ ,  $\hat{\mathbf{J}}^t \hat{\Omega} \hat{\mathbf{J}} = 0$  and  $\hat{\mathbf{G}}^t \hat{\Omega} \hat{\mathbf{H}} = 0$ . The derived conditions are necessary, nevertheless it is not clear that they are sufficient. By sufficient we mean that if a conic curve in the paracatadioptric image plane verifies these 3 constraints, then it is the locus where a certain line in the scene is projected. Notice that, neglecting the scale factor, the conic curve  $\bar{\Omega}$  provided by equation 3 is a function of 2 independent parameters. These 2 degrees of freedom (DOF) are associated with the pose of plane  $\Pi$  containing the original line and the effective viewpoint (Fig. 1). Since in general a conic curve has 5 DOF, then we must be able to find 3, and no more than 3, independent constraints. This proves the sufficiency of the statement.

### 3 Fitting a Conic Curve to Image Points

Assume the paracatadioptric image of a line in space. The line is projected in a conic curve  $\hat{\Omega}$  (equation 4). The conic curve  $\hat{\Omega}$  can be parameterized by a point  $\hat{\omega}$  in  $P^5$  [7]

$$\hat{\omega} = (a, b, c, d, e, f)^t \quad (5)$$

Consider the set of image points  $\hat{\mathbf{x}}_j = (\hat{x}_j, \hat{y}_j)^t$  with  $j = 1, 2 \dots M$ . If the points lie on conic  $\hat{\omega}$  then the equality of equation 6 must be verified. However equation 6 holds only in ideal circumstances. In general the data points  $\hat{\mathbf{x}}_j$  are corrupted with noise and  $\mathbf{A}\hat{\omega} \neq 0$ .

$$\underbrace{\begin{bmatrix} \hat{x}_1^2 & 2\hat{x}_1\hat{y}_1 & \hat{y}_1^2 & 2\hat{x}_1 & 2\hat{y}_1 & 1 \\ \hat{x}_2^2 & 2\hat{x}_2\hat{y}_2 & \hat{y}_2^2 & 2\hat{x}_2 & 2\hat{y}_2 & 1 \\ \vdots & \vdots & \vdots & \vdots & \vdots & \vdots \\ \hat{x}_M^2 & 2\hat{x}_M\hat{y}_M & \hat{y}_M^2 & 2\hat{x}_M & 2\hat{y}_M & 1 \end{bmatrix}}_{\mathbf{A}} \hat{\omega} = 0 \quad (6)$$

A conic fitting algorithm determines the curve that best fits the data accordingly to a certain distance metric. There

are several approaches to estimate a conic curve using image points [6]. They differ between each other by the criteria, or metric, that is minimized in the fitting process. This section reviews some well known conic fitting methods and compares their performance.

#### 3.1 Conic Fitting Methods

We focus exclusively on direct methods for which the fitting problem can be solved naturally by an eigensystem

##### 3.1.1 Linear Least Squares (LMS)

Consider the  $M \times 6$  design matrix  $\mathbf{A}$  provided in equation 6. The LMS method estimates the conic curve  $\hat{\omega}$  that minimizes the algebraic distance  $d = \hat{\omega}^t \mathbf{A}^t \mathbf{A} \hat{\omega}$  under the constraint  $\hat{\omega}^t \hat{\omega} = 1$ . The objective function is provided in equation 7 where the constraint is introduced using a Lagrange multiplier  $\lambda$

$$\phi_{lms}(\hat{\omega}, \lambda) = \hat{\omega}^t \mathbf{A}^t \mathbf{A} \hat{\omega} + \lambda(\hat{\omega}^t \hat{\omega} - 1) \quad (7)$$

The conic curve  $\hat{\omega}$  that minimizes  $\phi_{lms}$  is determined by solving the eigensystem  $\mathbf{A}^t \mathbf{A} \hat{\omega} = \lambda \hat{\omega}$ . The minimizer is the eigenvector corresponding to the smallest eigenvalue of matrix  $\mathbf{A}^t \mathbf{A}$ .

##### 3.1.2 Approximate Mean Squares (AMS)

The approximate mean square metric has been introduced by Taubin in [5]. The proposed conic fitting method minimizes the algebraic distance under the constraint  $\hat{\omega}^t (\mathbf{A}_x^t \mathbf{A}_x + \mathbf{A}_y^t \mathbf{A}_y) \hat{\omega} = 1$  where  $\mathbf{A}_x$  and  $\mathbf{A}_y$  are the partial derivatives of  $\mathbf{A}$ . The corresponding objective function is

$$\phi_{ams}(\hat{\omega}, \lambda) = \hat{\omega}^t \mathbf{A}^t \mathbf{A} \hat{\omega} + \lambda(\hat{\omega}^t (\mathbf{A}_x^t \mathbf{A}_x + \mathbf{A}_y^t \mathbf{A}_y) \hat{\omega} - 1) \quad (8)$$

The minima of equation 8 can be determined analytically by solving the generalized eigensystem  $\mathbf{A}^t \mathbf{A} \hat{\omega} = \lambda(\mathbf{A}_x^t \mathbf{A}_x + \mathbf{A}_y^t \mathbf{A}_y) \hat{\omega}$ . The conic curve estimation is provided by the eigenvector corresponding to the smallest eigenvalue.

##### 3.1.3 Direct Least Square Fitting of Ellipses (FF)

Since the conic  $\bar{\Omega}$  is a circle and the transformation  $\mathbf{H}_c$  is affine (equations 2 and 3), then the paracatadioptric image of a line  $\hat{\Omega}$  must be a circle/ellipse. The estimation method proposed in [4] is ellipse specific. Consider the following  $6 \times 6$  matrix

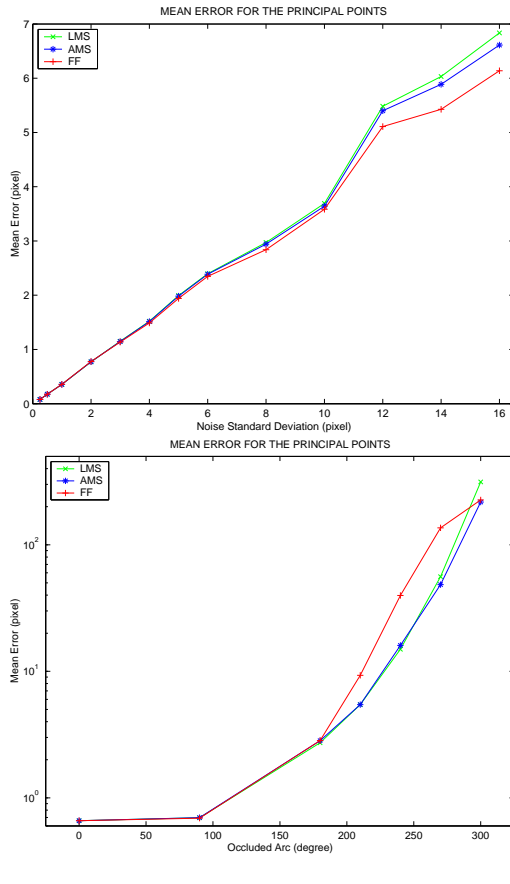


Figure 2: Comparing the performance of the conic fitting methods. Top: Robustness to noise without occlusion. Bottom: Robustness to occlusion in the presence of noise with standard deviation  $\sigma = 2$  (pixel)

$$\mathbf{C} = \begin{bmatrix} 0 & 0 & 2 & 0 & 0 & 0 \\ 0 & -1 & 0 & 0 & 0 & 0 \\ 2 & 0 & 0 & 0 & 0 & 0 \\ 0 & 0 & 0 & 0 & 0 & 0 \\ 0 & 0 & 0 & 0 & 0 & 0 \\ 0 & 0 & 0 & 0 & 0 & 0 \end{bmatrix}$$

If a conic  $\hat{\omega}$  verifies  $\hat{\omega}^t \mathbf{C} \hat{\omega} = 1$  then it must be a circle/ellipse. The conic fitting method proposed in [4] estimates the curve by minimizing the algebraic distance to the data points under the constraint  $\hat{\omega}^t \mathbf{C} \hat{\omega} = 1$ . The resultant objective function is provided below where the constraint is introduced using a Lagrange multiplier

$$\phi_{ff}(\hat{\omega}, \lambda) = \hat{\omega}^t \mathbf{A}^t \mathbf{A} \hat{\omega} + \lambda(\hat{\omega}^t \mathbf{C} \hat{\omega} - 1) \quad (9)$$

It can be proved that the conic  $\hat{\omega}$  which minimizes  $\phi_{ff}$  and verifies the constraint is the eigenvector corresponding to the single positive eigenvalue of the generalized eigen-system  $\mathbf{A}^t \mathbf{A} \hat{\omega} = \lambda \mathbf{C} \hat{\omega}$  [4].

### 3.2 Performance Evaluation

An arc of a test conic with pre-defined amplitude is uniformly sampled by 100 points. Two dimensional gaussian noise with zero mean and standard deviation  $\sigma$  is added to each sample. These samples are the data points used by the different estimators. The principal points of the estimated curve are compared with the ground truth and the mean error is computed over 100 runs of each experiment.

Consider the results depicted in Fig. 2. The graphic at the top shows the robustness to noise of the different methods. In this situation there is no occlusion and the entire conic is sampled. All the algorithms exhibit a similar graceful degradation in the presence of increasing noise. The FF method is the one that seems to be more robust. The graphic at the bottom shows the behavior in the presence of occlusion. The noise standard deviation is 2 pixels and the amplitude of the sampled arc decreases from 360° (the entire conic) up to 60° (occlusion of 300°). In all methods the estimation result suffers an abrupt degradation when the occlusion is higher than 220°. Nevertheless the AMS method seems to be the one that better deals with occlusion.

## 4 Direct Least Square Fitting of Paracatadioptric Line Images (CATPARB)

In general a conic has 5 degrees of freedom and can be parametrized by a point in  $P^5$ . Neglecting the scale factor the space of all conics has five dimensions. The approaches described in the previous section search the entire space for the conic that best fits the data. However not all conics can be the paracatadioptric image of a line. Consider points  $\hat{\mathbf{I}} = (i_x, i_y, i_z)^t$ ,  $\hat{\mathbf{J}} = (j_x, j_y, j_z)^t$ ,  $\hat{\mathbf{G}} = (g_x, g_y, g_z)^t$  and  $\hat{\mathbf{H}} = (h_x, h_y, h_z)^t$  introduced in section 2.2. As discussed a conic curve  $\hat{\omega}$  is the paracatadioptric projection of a line if, and only if,  $\Upsilon \hat{\omega}$  is null with  $\Upsilon$  the  $3 \times 6$  matrix provided in equation 10.

$$\underbrace{\begin{bmatrix} i_x^2 & 2i_x i_y & i_y^2 \\ j_x^2 & 2j_x j_y & j_y^2 \\ g_x h_x & g_x g_y + h_x h_y & g_y h_y \end{bmatrix}}_{\Upsilon} \begin{bmatrix} 2i_x i_z & i_z^2 \\ 2j_x j_z & j_z^2 \\ g_x g_z + h_x h_z & g_y g_z + h_y h_z & g_z h_z \end{bmatrix} \hat{\omega} = 0 \quad (10)$$

The paracatadioptric line image  $\hat{\omega}$  must lie in the null space of matrix  $\Upsilon$ . The null space of  $\Upsilon$  is a linear subspace in the space of all conic curves. Our approach fits the data to the conic curve, lying in this subspace, that minimizes

the algebraic distance to the image points. Consider the singular value decomposition of matrix  $\Upsilon$ .

$$\Upsilon = \mathbf{U} \mathbf{S} \mathbf{V}^t$$

Matrices  $\mathbf{U}$ ,  $\mathbf{S}$  and  $\mathbf{V}$  have respectively dimension  $3 \times 3$ ,  $3 \times 6$  and  $6 \times 6$ .  $\mathbf{V}$  is full rank and orthonormal ( $\mathbf{V}^{-1} = \mathbf{V}^t$ ). The three last columns of  $\mathbf{V}$  are an orthonormal basis of the null space of  $\Upsilon$ . Consider the change on the base of representation  $\hat{\omega}_v = \mathbf{V}\hat{\omega}$ . If  $\hat{\omega}$  belongs to the null space of matrix  $\Upsilon$ , then the corresponding  $\hat{\omega}_v$  has the following structure

$$\hat{\omega}_v = (0, 0, 0, \underbrace{d_v, e_v, f_v}_{\rho})^t \quad (11)$$

The algebraic distance between conic  $\hat{\omega}$  and the data points is  $d = \hat{\omega}^t \mathbf{A}^t \mathbf{A} \hat{\omega}$ . Rewriting the algebraic distance in terms of the new coordinates arises  $d = \hat{\omega}_v^t \mathbf{V} \mathbf{A}^t \mathbf{A} \mathbf{V}^t \hat{\omega}_v$ . Taking into account the structure of  $\hat{\omega}_v$  (equation 11) comes that  $d = \rho^t \Lambda^t \Lambda \rho$  with  $\Lambda$  the bottom right  $3 \times 3$  submatrix of  $\mathbf{V} \mathbf{A}^t \mathbf{A} \mathbf{V}^t$ . We aim to determine the solution  $\rho$  which minimizes the algebraic distance  $d$  under the constraint  $\rho^t \rho = 1$ . The objective function is

$$\phi(\rho, \lambda) = \rho^t \Lambda^t \Lambda \rho + \lambda(\rho^t \rho - 1) \quad (12)$$

The minima of the objective function  $\phi$  is the eigenvector of matrix  $\Lambda^t \Lambda$  corresponding to the smallest eigenvalue. The final conic  $\hat{\omega}$  is computed by replacing  $\rho$  in equation 11 and making  $\hat{\omega} = \mathbf{V}^t \hat{\omega}_v$ .

## 5 Experiments

Accordingly to the results presented in section 3.2, the FF algorithm has the best performance in the presence of noise and the AMS method is the most robust to occlusion. The present section compares these two methods with the proposed CATPARB algorithm. Notice however that, while the FF and AMS conic fitting methods are generic, the CATPARB algorithm is specific to estimate the conic curves where lines in the scene are mapped by a paracatadioptric camera. We start by describing the simulation scheme used to generate artificial data. The performance of the AMS, FF and CATPARB methods in estimating paracatadioptric line images is compared. Experiments using real images are also presented

### 5.1 Simulation Scheme

Assume a paracatadioptric system with a field of view (FOV) of  $180^\circ$ . The paracatadioptric image of a line is generated as follows. As depicted in Fig. 1 to a line in the scene

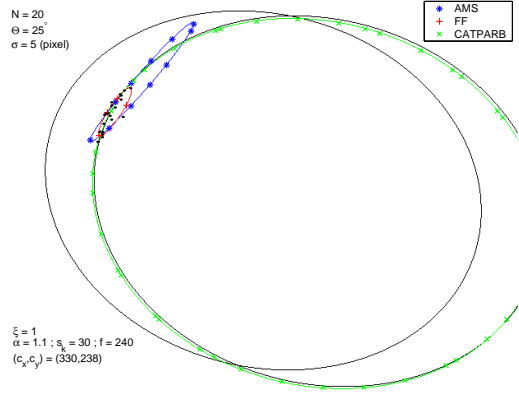


Figure 3: Estimating paracatadioptric line image using different methods

corresponds a plane  $\Pi$  with normal  $\mathbf{n}$ . The normal is unitary and randomly chosen from an uniform distribution in the sphere. Each normal defines a plane that intersects the unit sphere in a great circle. Notice that half of the great circle is within the camera field of view (the FOV is  $180^\circ$ ). An angle  $\theta$ , less or equal to the FOV, is chosen to be the amplitude of the arc that is actually visible in the paracatadioptric image. The arc is randomly and uniformly positioned along the part of the great circle which is within the FOV. The visible arc is uniformly sampled by a fixed number  $N$  of sample points. The each sample point corresponds a projective ray  $\mathbf{x}$ . The sample rays are projected using equation 1 and transformed using 2 with the chosen intrinsic parameters. Two dimensional gaussian noise with zero mean and standard deviation  $\sigma$  is added to each image point  $\hat{\mathbf{x}}$ . Fig. 3 is an example of a simulated image of a randomly generated paracatadioptric line image. The visible arc has an amplitude of  $25^\circ$  and is sampled by 20 points. The gaussian noise added to the samples has a standard deviation of 5 pixels. As a final remark notice that the amplitude of the visible arc is measured in the great circle where plane  $\Pi$  intersects the sphere, and not in the conic curve where the line is projected. In general the visible angle of the paracatadioptric line image is much less than  $\theta$ .

### 5.2 Comparing AMS, FF and CATPARB Methods

Consider the first graphic on Fig. 4 which compares the performance of the three methods. The data points are artificially generated using the simulation scheme described above. An arc with an amplitude  $80^\circ$  is uniformly sampled by 40 points. Each method fits a conic curve to the data points. The estimated conic is compared with the ground truth and the RMS error in the principal points is computed

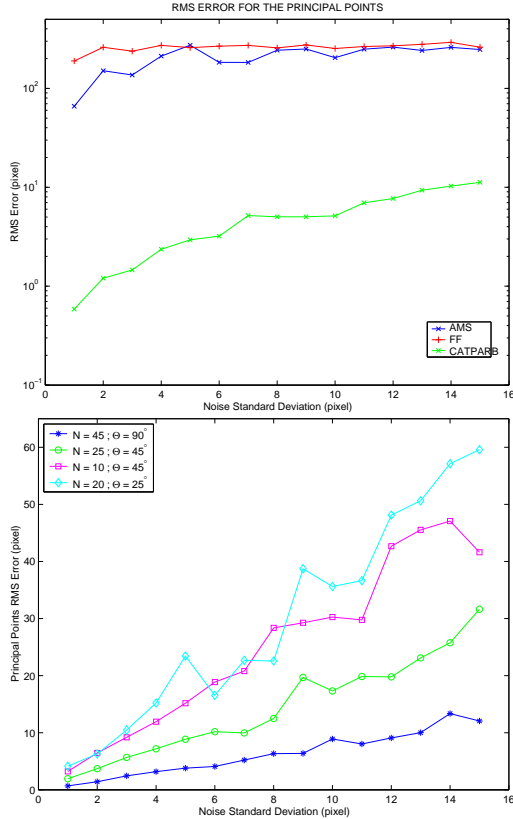


Figure 4: Estimation of paracatadioptric line images. Top: The performance of AMS, FF and CATPARB methods ( $N = 40$ ,  $\theta = 80^\circ$ ). Bottom: The performance of the CATPARB algorithm.

over 100 runs of each experiment. The estimation results dramatically improve when using the CATPARB algorithm. The graphic at the bottom of Fig. 4 shows the behavior of the proposed approach in the presence of increasing noise for different values of  $N$  and  $\theta$ . As expected the performance is worse when the number of samples and/or the amplitude of the visible arc decrease.

### 5.3 Experiments with Real Images

Fig. 5 shows a calibrated paracatadioptric image with resolution  $1704 \times 2272$ . The conic curve where a line is projected has only 2 independent degrees of freedom (proposition in section 2.2). Thus two image points are enough to correctly determine a paracatadioptric line image. We have selected by hand two points lying on the conic locus where a certain line in the scene is projected. The estimation results using the proposed CATPARB algorithm can be observed in Fig. 5. Notice that in general a conic curve can only be estimated using 5 or more data points.

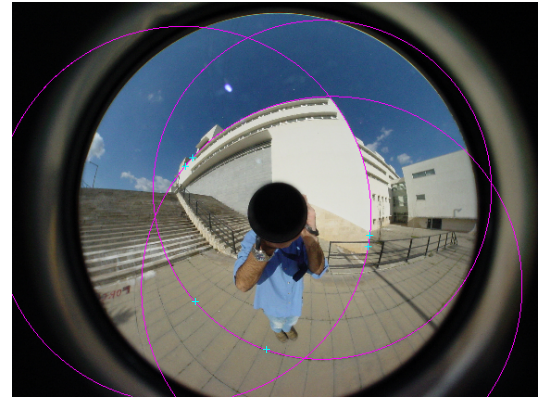


Figure 5: Estimating lines in a real image. The crosses are the points selected by hand

## 6 Summary and Conclusions

The article presents a specific method to estimate lines in calibrated paracatadioptric images. The algorithm uses the properties of parabolic image formation to constrain the search space. The performance of the proposed approach is compared with other generic conic fitting methods using both simulated data and real images.

## References

- [1] S. Baker and S. Nayar, "A theory of catadioptric image formation," in *Proc. of IEEE International Conference on Computer Vision*, Bombay, 1998, pp. 35 – 42.
- [2] Joao P. Barreto and Helder Araujo, "Geometric properties of central catadioptric line images," in *Proc. of European Conference on Computer Vision*, Copenhagen, Denmark, May 2002.
- [3] C. Geyer and K. Daniilidis, "Paracatadioptric camera calibration," *IEEE Trans. on Pattern Analysis and Machine Intelligence*, vol. 24, no. 4, April 2002.
- [4] A. Fitzgibbon, M. Pilu and R. Fisher, "Direct Least Squares Fitting of Ellipses," *IEEE Trans. on Pattern Analysis and Machine Intelligence*, vol. 21, no. 5, May 1999.
- [5] G. Taubin, "Estimation of Planar Curves, Surfaces and Non-planar Space Curves Defined by Implicit Equations," *IEEE Trans. on Pattern Analysis and Machine Intelligence*, vol. 13, no. 11, November 1991.
- [6] Z. Zhang, "Parameter estimation techniques: A tutorial with application to conic fitting," *INRIA Raport de Recherche n 2676*, October 1995.
- [7] J. G. Semple and G. T. Kneebone, *Algebraic Projective Geometry*, Clarendon Press, 1998.